tvst

Glaucoma

Inhibition of TGF-β2–Induced Trabecular Meshwork Fibrosis by Pirfenidone

Xiaofeng Zhu[1], Bei Zeng[1], Caiqing Wu[1], Zidong Chen[1], Minbin Yu[1], and Yangfan Yang[1]

[1] State Key Laboratory of Ophthalmology, Zhongshan Ophthalmology Center, Sun Yat-Sen University, Guangdong Provincial Key Laboratory of Ophthalmology and Visual Science, Guangzhou, China

Correspondence: Yangfan Yang, State Key Laboratory of Ophthalmology, Zhongshan Ophthalmology Center, Sun Yat-Sen University, 7 Jinsui Road, Clinical Building Room 1701, Guangzhou 510060, China. e-mail: yangyangfan@gzzoc.com

Received: July 5, 2023
Accepted: September 25, 2023
Published: November 17, 2023

Keywords: pirfenidone; trabecular meshwork; fibrosis; glaucoma

Citation: Zhu X, Zeng B, Wu C, Chen Z, Yu M, Yang Y. Inhibition of TGF-β2–induced trabecular meshwork fibrosis by pirfenidone. Transl Vis Sci Technol. 2023;12(11):21, https://doi.org/10.1167/tvst.12.11.21

Purpose: Trabecular meshwork (TM) fibrosis is a crucial pathophysiological process in the development of primary open-angle glaucoma. Pirfenidone (PFD) is a new, broad-spectrum antifibrotic agent approved for the treatment of idiopathic pulmonary fibrosis. This study investigated the inhibitory effect of PFD on TM fibrosis and evaluated its efficacy in lowering intraocular pressure (IOP).

Methods: Human TM cells were isolated, cultured, and characterized. Cell Counting Kit-8 was used to evaluate the proliferation and toxicity of different concentrations of PFD on normal or fibrotic TM cells. TM cells were treated with transforming growth factor beta-2 (TGF-β2) in the absence or presence of PFD. Western blotting and immunofluorescence analyses were used to analyze changes in the TM cell cytoskeleton and extracellular matrix (ECM) proteins, including alpha-smooth muscle actin (α-SMA), F-actin, collagen IV (COL IV), and fibronectin (FN). An ocular hypertension (OHT) mouse model was induced with Ad-TGF-$\beta2^{C226/228S}$ and then treated with PFD or latanoprost (LT) eye drops to confirm the efficacy of PFD in lowering IOP.

Results: PFD inhibited the proliferation of fibrotic TM cells in a dose-dependent manner and inhibited TGF-β2–induced overexpression of α-SMA, COL IV, and FN in TM cells. PFD stabilized F-actin. In vivo, PFD eye drops reduced the IOP of the OHT models and showed no significant difference compared with LT eye drops.

Conclusions: PFD inhibited TGF-β2–induced TM cell fibrosis by rearranging the disordered cytoskeleton and decreasing ECM deposition, thereby enhancing the aqueous outflow from the TM outflow pathway and lowering IOP, which provides a potential new approach to treating glaucoma.

Translational Relevance: Our work with pirfenidone provides a new approach to treat glaucoma.

Introduction

Primary open-angle glaucoma (POAG) is an optic neuropathy characterized by irreversible retinal ganglion cell damage and visual field loss.[1] The main risk factor is the pathological elevation of intraocular pressure (IOP), caused by increased resistance to aqueous humor outflow due to functional and structural damage of the trabecular meshwork (TM). Lowering the IOP is the only effective way to stop or slow the progression of glaucoma.[2]

In glaucoma, transforming growth factor beta (TGF-β) is significantly elevated in the aqueous humor, and the level of biologically active TGF-β2 is higher in the aqueous humor of eyes with POAG than that with primary angle-closure glaucoma.[3–6] TGF-β acts by inducing the transformation of TM cells into myofibroblast-like structures, increasing the cross-linked actin networks (CLANs) and extracellular matrix (ECM) accumulation, increasing oxidative stress, accelerating apoptosis and cell aging, rendering TM cells fibrotic, and increasing aqueous humor outflow resistance.[7–10] TM fibrosis plays an important role in the development of POAG.

Currently, the main mechanism of clinical ocular hypotensives is to reduce aqueous humor production of the ciliary body or increase aqueous humor outflow through the uveoscleral pathway. In clinical practice, it has been observed that some glaucoma patients who

have been using currently available ocular hypotensives for some time may experience a rise in IOP or fail to achieve the target IOP reduction, which may be attributed to the persistent chronic fibrosis of the TM. Reversing TM fibrosis to improve aqueous humor outflow from the TM pathway is a feasible treatment method for reducing IOP. However, only Rho-kinase inhibitors have been used successfully in clinical settings.[11]

Pirfenidone (PFD) is a new broad-spectrum antifibrotic agent approved for the treatment of idiopathic pulmonary fibrosis[12] that offers safety, efficacy, and low toxicity. Our team has demonstrated that PFD can effectively inhibit the proliferation, migration, differentiation, and collagen contraction of human ocular Tenon's fibroblasts, and the effective concentration was not toxic to the ocular surface and intraocular tissues.[13] PFD can also inhibit proliferation-related ocular diseases, such as proliferative vitreoretinopathy, and those that occur after cataract.[14,15] Furthermore, PFD suppresses ECM deposition in fibroblasts from intraconal orbital fat tissues in vitro.[16] Therefore, PFD is a good prospect for TM anti-fibrosis treatment.

In this study, we first investigated the effect of PFD on TGF-β2–induced TM cell fibrosis in vitro, including its effects on cytoskeleton and ECM. Second, we utilized an adenovirus 5 (Ad5) viral vector to overexpress a bioactive form of human TGF-β2 in the TM of mouse eyes (Ad-TGF-$\beta2^{C226/228S}$), to establish ocular hypertension (OHT) mouse models.[17,18] We examined whether PFD reduced IOP induced by Ad-TGF-$\beta2^{C226/228S}$ in OHT mouse models.

Methods

Human TM Cell Isolation and Culture

The materials used to isolate human primary trabecular meshwork (pTM) cells were obtained from the corneoscleral rings after keratoplasty and were provided by Gu Jianjun's team at the Zhongshan Ophthalmology Center of Sun Yat-Sen University. This study was approved by the hospital's ethics committee. The corneoscleral rings including TM tissue were cut into 1- to 2-mm^2 tissue blocks, cultured on six-well plates (Thermo Fisher Scientific, Waltham, MA) containing Dulbecco's Modified Eagle Medium/Nutrient Mixture F-12 (DMEM/F-12; Thermo Fisher Scientific), 10% fetal bovine serum, and 1% penicillin/streptomycin at 37°C with 5% CO_2. The obtained cells were treated with 100-nM dexamethasone (DEX; Sigma-Aldrich, St. Louis, MO) for 7 days to stimulate myocilin production, which is a reliable marker of human TM cells and can be assessed via western blot analysis (Fig. 1).[7,19] All subsequent experiments were biological replicates, using TM cells isolated from different donors.

Cell Proliferation Assay

To determine the effects of PFD on the proliferation of TM cells, various concentrations of PFD were used to treat TM cells, which were then assayed using Cell Counting Kit-8 (CCK-8; (Dojindo Laboratories, Tabaru, Japan) according to the manufacturer's instructions. Pirfenidone (TCI, Shanghai, China) was dissolved in phosphate-buffered saline (PBS) at a temperature of 65°C, which was then added into a complete medium to obtain the following concentrations: 0.05, 0.1, 0.2, 0.4, 0.8, and 1.0 mg/mL. TM cell suspensions were seeded in a 96-well plate (100 µL, 1 × 10^4 cells/well; Thermo Fisher Scientific) and incubated overnight. The plates were then divided into three groups. Group 1 was cultured with 0, 0.05, 0.1, 0.2, 0.4, 0.8, and 1.0 mg/mL of PFD for 24 hours (Fig. 2A). Group 2 cells were co-treated with 10 ng/mL human TGF-β2 (PeproTech, Cranbury, NJ) and PFD for 24 hours to simulate early-stage fibrotic TM cells (Fig. 2B). Group 3 was initially treated with TGF-β2 alone for 24 hours to simulate late-stage fibrotic TM

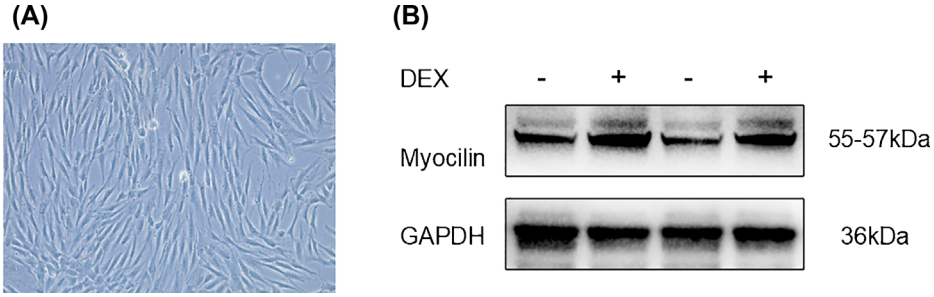

Figure 1. Identification of trabecular meshwork cells. (**A**) TM cells of passage 3. (**B**) Overexpression of myocilin after DEX treatment for 7 days in TM cells.

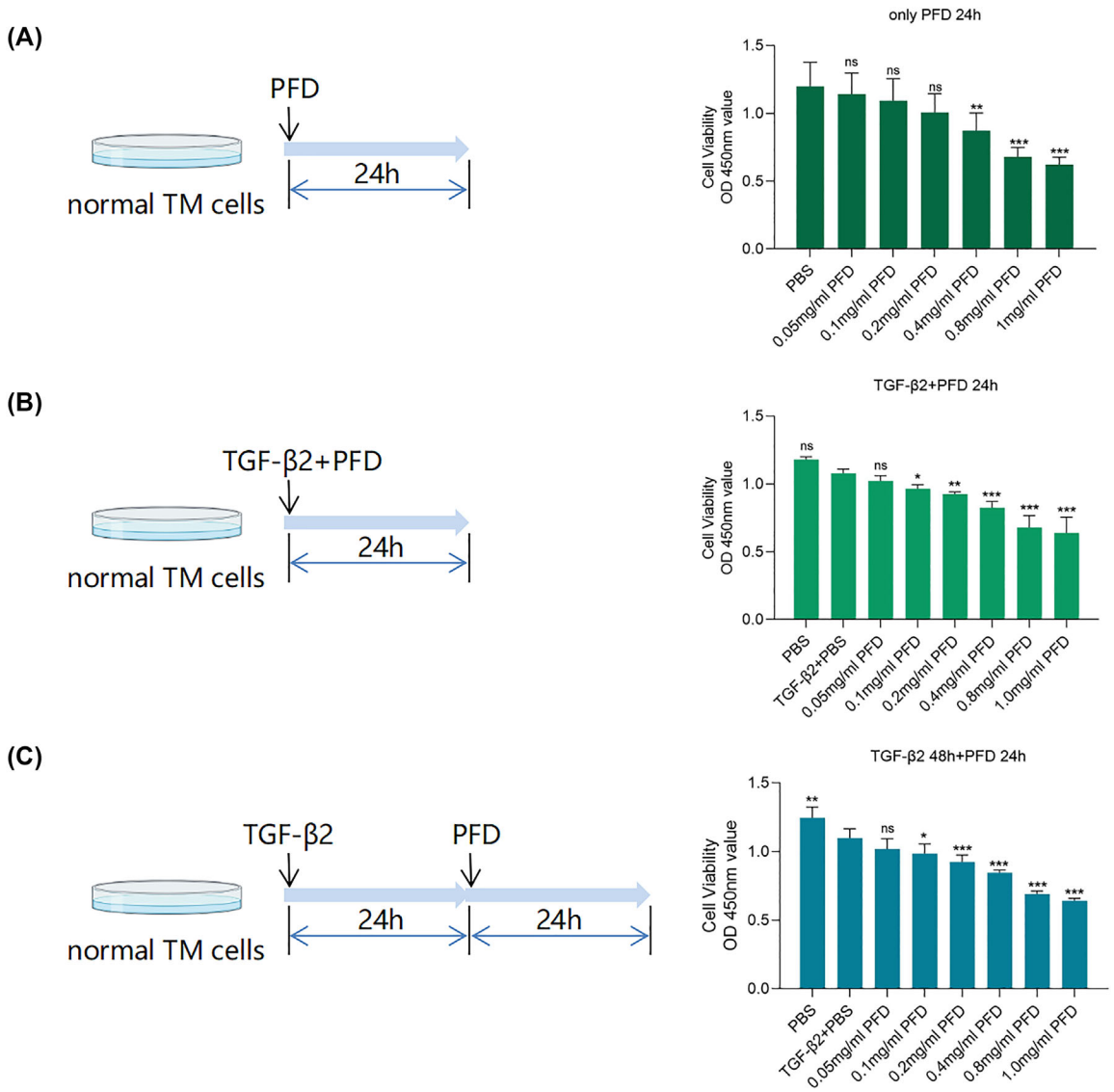

Figure 2. Proliferation of TM cells measured by CCK-8 to determine the relative number of cells. (**A**) Group 1, normal TM cells treated with PFD for 24 hours. (**B**) Group 2, normal TM cells co-treated with 10 ng/mL TGF-β2 and PFD for 24 hours to simulate the early stage. (**C**) Group 3, normal TM cells treated with 10 ng/mL TGF-β2 for 24 hours and then with PFD for 24 hours to simulate the late stage. The *bars* and *error bars* indicate the mean ± SD. Significance was determined by one-way ANOVA with Tukey's multiple comparisons test ($n = 5$). *$P < 0.05$, **$P < 0.01$, ***$P < 0.001$. ns, not significant.

cells and the culture was incubated after the addition of PFD for another 24 hours (Fig. 2C). After incubation, 10 µL of CCK-8 was added to each well of the plates. The plates were incubated for 1.5 hours at 37°C, and the absorbance at 450 nm was measured using a microplate reader.

Western Blot Analysis

Cell suspensions were seeded in six-well plates and incubated overnight. Cells were processed as early stage and late stage. The concentrations of PFD were 0.1 mg/mL and 0.2 mg/mL. TM cells were lysed using a total protein extraction kit (KeyGEN BioTECH, Nanjing, China) on ice. Protein concentrations were measured using a BCA Protein Assay Kit (GlpBio, Montclair, CA). The protein solution and loading buffer were boiled together at a ratio of 4:1 for 10 minutes at 100°C before loading. Protein solutions were separated by electrophoresis and transferred onto polyvinylidene fluoride membranes (MilliporeSigma, St. Louis, MO). The membrane was blocked with western rapid blocking solution for 15 minutes and exposed to primary antibodies overnight at 4°C. Next,

Table. Primary Antibodies Used in Western Blot and Immunocytochemistry

Antibodies	Western Blot	Immunocytochemistry	Supplier, Catalog No.
Anti-myocilin	1:2000	—	Proteintech, 60357
Anti-α-SMA	1:10000	1:500	Abcam, ab124964
Anti-F-actin	1:500	1:500	Abcam, ab130935
Anti-collagen IV	1:1000	1:500	Abcam, ab6586
Anti-fibronectin	1:1000	1:500	Abcam, ab2413

the membranes were incubated with goat anti-rabbit or anti-mouse secondary antibodies, imaged with a Bio-Rad ChemiDoc Imaging System (Bio-Rad, Hercules, CA) and analyzed using ImageJ (National Institutes of Health, Bethesda, MD). All primary antibody parameters are listed in the Table.

Immunocytochemistry Analysis

The cell suspensions were seeded on 14-mm-diameter cell coverslips and incubated overnight. The cells were processed as described above. The coverslips were fixed with 4% paraformaldehyde (Biosharp, Anhui, China) at room temperature (RT) for 15 minutes, rinsed three times in PBS, and permeabilized with 0.5% Triton X-100 (MP Biomedicals, Santa Ana, CA) for 15 minutes and then rinsed again. The coverslips were incubated in 10% goat serum albumin (Boster Bio, Pleasanton, CA) for 1 hour, then incubated overnight at 4°C with primary antibodies. The coverslips were then incubated with secondary antibodies for 1 hour at RT in the dark. Nuclei were stained with ProLong Gold Antifade Reagent and 4′,6-diamidino-2-phenylindole (DAPI; (Cell Signaling Technology, Danvers, MA). The coverslips were observed under a fluorescence microscope (Axio Imager.Z29; Zeiss Microsystems, Wetzlar, Germany). The concentrations of the antibodies used in the experiment are shown in the Table.

Animals

All animals were treated in accordance with the tenets of the Declaration of Helsinki and in compliance with the ARVO Statement for the Use of Animals in Ophthalmic and Vision Research. All of the experiments were approved by the Institutional Animal Care and Use Committee (IACUC) of the Zhongshan Ophthalmology Center of Sun Yat-Sen University (Z2022047). Healthy C57BL/6J mice (6–8 weeks old; male; weight, 20–25 g) were used. The mice were purchased from Guangdong Vital River Laboratory Animal Technology Co., Ltd. (Guangzhou, China), housed in clear cages, and kept in housing rooms at 21°C with a 12-hour:12-hour light:dark cycle.

OHT Animal Model and Drug Treatments

The first step was to establish an OHT mouse model. All mice were intraperitoneally anesthetized with avertin (0.2 mL/10 g). Proparacaine hydrochloride eye drops (Alcon Couvreur NV, Puurs, Belgium) were used for ocular surface anesthesia. The vitreous of one eye of each mouse in the OHT model group was injected with 2.5 µL of 1×10^8 pfu/mL Ad-TGF-$\beta 2^{C226/228S}$ carrying red fluorescent labels (Dongze-bio Co., Guangzhou, China); mice in the control group were injected with 2.5 µL of 1×10^8 pfu/mL Ad-Null. All mice were administered tobramycin–dexamethasone eye ointment once after intravitreal injection. The IOP was measured every 3 days for 5 weeks to observe whether the OHT mouse model had been successfully established.

The second step was treatment in vivo. Some mice were injected intravitreally with Ad-TGF-$\beta 2^{C226/228S}$ monocularly, and the control group was injected with Ad-Null. IOP was measured once on days 1, 7, and 14. The Ad-TGF-$\beta 2^{C226/228S}$–injected mice were further divided into three groups at day 14: (1) PBS treatment, (2) 0.4% PFD–hydroxypropyl methyl cellulose (HPMC) eye drops (2 mL 20 mg/mL PFD + 3 mL PBS + 5 mL HPMC), and (3) latanoprost (LT) eye drops (Taejoon Pharm Co., Seoul, Korea). The control group was given PBS. All groups were dosed twice a day at 8 AM and 6 PM, and IOP measurements were recorded every 3 days.

IOP Measurement

All mice were anesthetized intraperitoneally. The IOP was measured using an iCare TONOLAB tonometer (iCare Finland Oy, Vantaa, Finland). Each recorded IOP was the average of six measurements, and three IOP readings were recorded in the same eye to calculate the mean value. In the first step of the exper-

iment, IOP measurements were continued for 5 weeks. In the second step, the experiment lasted for 1 month.

Image Analysis

ImageJ 1.53f51 was used to quantify the positively stained cells, as indicated by the blue color due to DAPI and green signals from the secondary antibodies. We defined the positive area of a single cell as the total positive area divided by the number of nuclei. The number of nuclei was counted by ImageJ, and marginal nuclei were excluded.

Statistical Analysis

Individual sample sizes are specified in each figure caption. Data analysis was conducted using SPSS Statistics 22.0 (IBM, Chicago, IL) and Prism 9.0 (GraphPad, San Diego, CA). All data are presented as mean ± standard deviation (SD). For data among multiple groups, a one-way or two-way analysis of variance (ANOVA) with Tukey's multiple comparison test was used. Statistical significance was set at $P < 0.05$.

Results

TM Cell Characterization

pTM cells isolated from the corneal rims were cultured for three to five passages and were used in the experiments.[19] The TM cells of passages three to five had an elongated, spindle-shaped morphology with many overlapping processes (Fig. 1A).[20] On western blotting, the overexpression of myocilin induced by DEX was indicated by a doublet (Fig. 1B) at 55 to 57 kDa,[19,20] which confirmed that the obtained cells were TM cells.

PFD Inhibited the Proliferation of TM Cells in a Dose-Dependent Manner

The CCK-8 assay showed that PFD reduced TM cell proliferation and viability in a dose-dependent manner. We observed that 0.4 mg/mL PFD significantly inhibited the growth of normal TM cells (Fig. 2A). TGF-β2 inhibited TM cells in a time-dependent manner (Figs. 2B, 2C). Furthermore, it was demonstrated that 0.1 mg/mL PFD could significantly inhibit the proliferation of fibrotic TM cells induced by TGF-β2, regardless of whether the fibrosis is in its early or late stage (Figs. 2B, 2C). The higher the concentration of PFD, the more pronounced the inhibition. Based on the results of the CCK-8 assay, we determined that 0.2 mg/mL PFD was the safest and most effective concentration for subsequent experiments, and 0.1 mg/mL PFD was used for comparison purposes.

Effects of PFD on Early-Stage Fibrotic TM Cells Induced by TGF-β2

We performed a quantitative evaluation of TGF-β2–induced TM fibrosis and the antifibrotic effect of PFD using western blotting. The results indicated that the levels of alpha-smooth muscle actin (α-SMA) and collagen IV (COL IV) were upregulated in TM cells after TGF-β2 treatment (Figs. 3B, 3C, 3F, 3G), whereas F-actin and fibronectin (FN) tended to increase; however, the difference was not significant (Figs. 3A, 3D, 3E, 3H). PFD inhibited the expression of α-SMA, COL IV, and FN in early-stage fibrotic TM cells, the levels of which were approximately baseline or below, and the effect of 0.2 mg/mL PFD was more significant than that of 0.1 mg/mL PFD (Figs. 3F–3H). PFD does not affect F-actin levels in early-stage fibrotic TM cells.

Effects of PFD on Late-Stage Fibrotic TM Cells Induced by TGF-β2

In the late fibrosis environment, we found that the fibrotic marker α-SMA was significantly upregulated in TM cells by TGF-β2 exposure (Figs. 4B, 4F) and that COL IV (Figs. 4C, 4G) and FN (Figs. 4D, 4H) were overexpressed. TGF-β2 induced an upward trend in the expression of F-actin, but it was not significant (Figs. 4A, 4E). However, the addition of pirfenidone inhibited the expression of F-actin and showed a lower trend than the control group in late-stage fibrotic TM cells. In particular, the 0.2-mg/mL concentration of PFD demonstrated better efficacy compared to 0.1 mg/mL (Fig. 4E). α-SMA expression was not significantly reduced by 0.1 mg/mL PFD; however, it was significantly reduced by 0.2 mg/mL PFD (Fig. 4F). Similarly, PFD inhibited COL IV and FN formation induced by TGF-β2 (Figs. 4G, 4H). We also found that PFD reduced the expression of these proteins to approximately baseline or below levels, despite the 48-hour TGF-β2 effect.

PFD Remodeled the Cytoskeleton of Fibrotic TM Cells

We observed that normal TM cells exposed to TGF-β2 for 24 hours had scrambled and overlapping F-

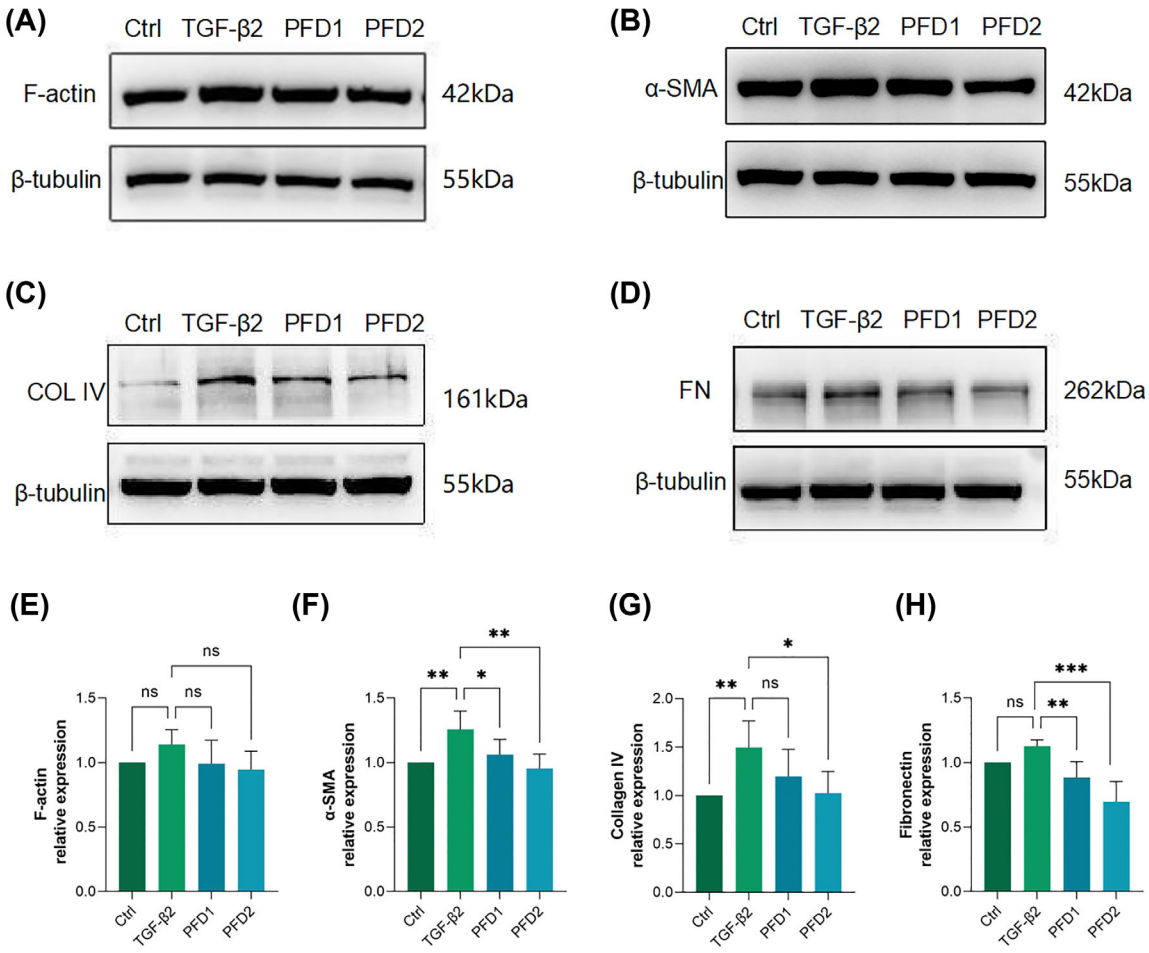

Figure 3. Effects of pirfenidone on early-stage fibrotic TM cells induced by TGF-β2. (**A**–**D**) Immunoblot of F-actin (**A**), α-SMA (**B**), COL IV (**C**), and FN (**D**) expression induced by TGF-β2 (10 ng/mL) with or without exposure to PFD for 24 hours. (E–H) Quantitative analysis of the expression of F-actin (**E**), α-SMA (**F**), COL IV (**G**), and FN (**H**) in early-stage fibrotic TM cells treated with PFD. Significance was determined by one-way ANOVA with Tukey's multiple comparisons test ($n = 5$). *$P < 0.05$, **$P < 0.01$, ***$P < 0.001$. PFD1, 0.1 mg/mL PFD; PFD2, 0.2 mg/mL PFD; ns, not significant.

actin compared to the control (Fig. 5A). We divided the total fluorescence area by the total nuclei to obtain the average positive area per cell, which indicated the protein expression of individual cells. We found that F-actin was still not significantly different in early-stage fibrotic TM cells; however, F-actin expression was significantly inhibited by co-treatment with 0.2 mg/mL PFD (Fig. 5B), and structural arrangement became orderly (Fig. 5A). In the late fibrotic environment, the cell bodies of TM cells exposed to TGF-β2 were larger than those of early-stage fibrotic cells; TM cells had the appearance of denser groups of actin bundles with a multidirectional orientation and overlaps, and the average positive area per cell was significantly different (Fig. 5E). This finding may be related to the duration of TGF-β2 treatment. Conversely, PFD had no obvious effect on the mean F-actin–positive area (Fig. 5F); however, it appeared that the F-actin arrangement was more ordered compared to the TGF-β2 group alone (Fig. 5E). This suggests that PFD stabilized the cytoskeleton of early-stage fibrotic TM cells or partially stabilized the cytoskeleton of late-stage cells.

Consistent with the western blot results, the fibrotic marker α-SMA was observed to be denser and thicker in fibrotic TM cells exposed to TGF-β2 (Fig. 5C). The longer the exposure to TGF-β2, the more obvious the effect. TM cells treated with TGF-β2 for 48 hours showed enlarged cell bodies and nuclei, thickened and disordered cytoskeletons, and no spindle morphology (Fig. 5G). Compared with F-actin, the effect of PFD on the inhibition of α-SMA stress fiber formation induced by TGF-β2 was even more pronounced in both early- and late-stage fibrotic TM cells (Figs. 5D, 5H). Similarly, the effect of PFD on remodeling was more pronounced in the early stages than in the late stages. The above results indicate that PFD reshaped the cytoskeleton of fibrotic TM cells, with a greater effect in the early stage than in the late stage, and it offered

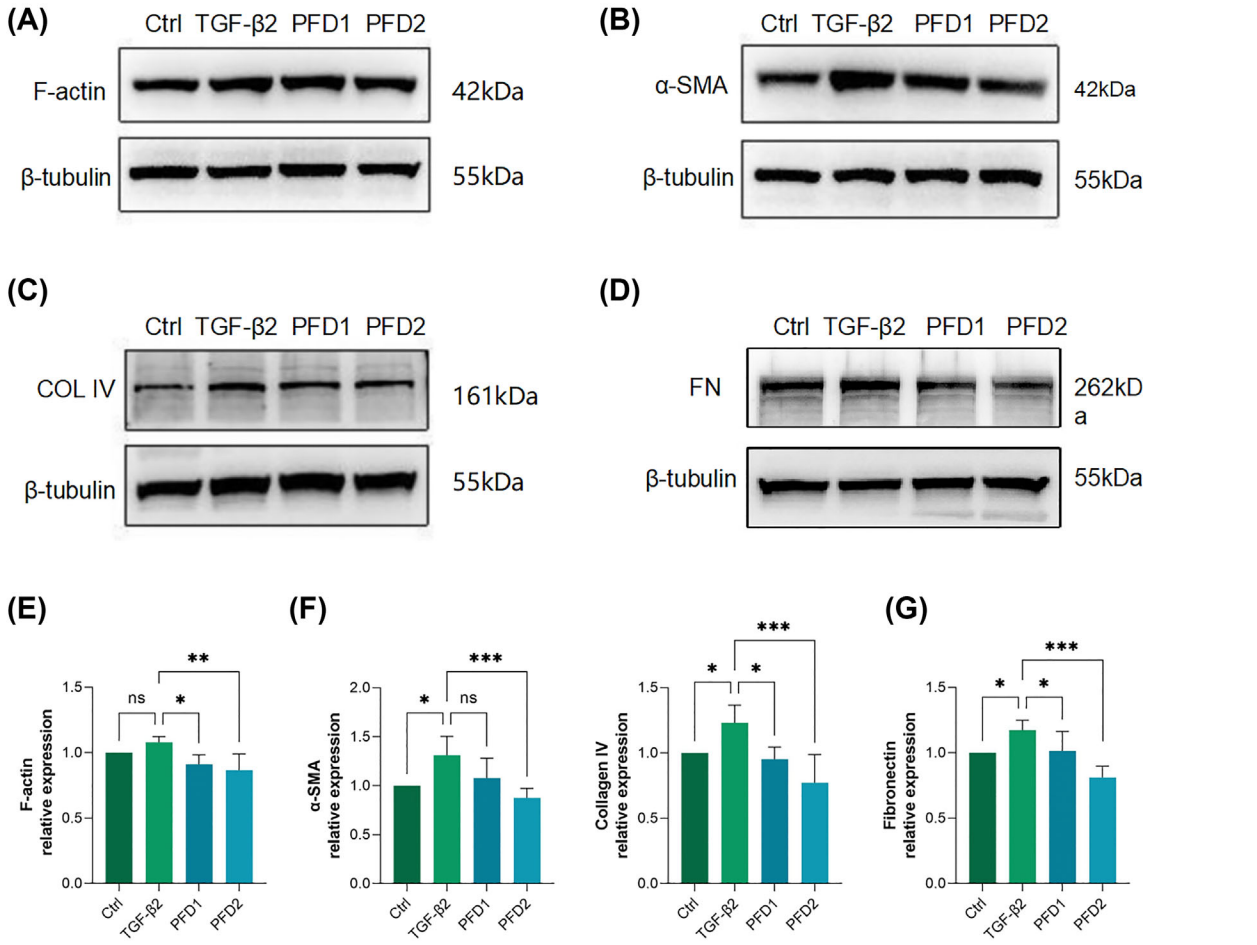

Figure 4. Effects of pirfenidone on late-stage fibrotic TM cells induced by TGF-β2. (**A**–**D**) Immunoblot of F-actin (**A**), α-SMA (**B**), COL IV (**C**), and FN (**D**) expression induced by TGF-β2 (10 ng/mL) with or without exposure to PFD for 48 hours. (**E**–**H**) Quantitative analysis of the expression levels of F-actin (**E**), α-SMA (F), COL IV (**G**), and FN (**H**) in late-stage fibrotic TM cells treated with PFD. Significance was determined by one-way ANOVA with Tukey's multiple comparisons test ($n = 5$). *$P < 0.05$, **$P < 0.01$, ***$P < 0.001$. PFD1, 0.1 mg/mL PFD; PFD2, 0.2 mg/mL PFD; ns, not significant.

several advantages in inhibiting α-SMA compared with F-actin.

PFD Reduced the ECM Deposition of Fibrotic TM Cells

In addition to affecting the cytoskeleton of the TM cells, TGF-β2 promoted deposition of ECM components (COL IV and FN) (Fig. 6). TGF-β2 prompted the secretion of COL IV (Fig. 6A) and the formation of dense FN (Fig. 6C) networks in early-stage fibrotic TM cells. Significant increases in the average positive area per cell were observed for COL IV (Fig. 6B) and FN (Fig. 6D). The same result was observed for the TGF-β2 group after 48 hours and even longer (Figs. 6E–6H). Co-treatment with TGF-β2 and PFD significantly decreased COL IV in early-stage fibrotic TM cells compared to treatment with TGF-β2 alone, approximating baseline levels (Fig. 6B). Similarly, PFD significantly decreased TGF-β2–stimulated FN areas; however, the levels remained significantly higher than those in the controls (Fig. 6D). In the late fibrotic environment, exposure to PFD resulted in a significant reduction in TGF-β2–induced COL IV and FN deposition. Similarly, the efficacy of PFD was more pronounced at a concentration of 0.2 mg/mL compared to 0.1 mg/mL (Figs. 6F, 6H).

Ad-TGF-$\beta2^{C226/228S}$ Successfully Induced OHT Mouse Models

Immunofluorescence analysis showed that Ad-TGF-$\beta2^{C226/228S}$ successfully targeted the trabecular meshwork of mice (Fig. 7A). The mean baseline IOP was 12.0 $\pm$ 1.5 mmHg in the OHT group ($n = 10$) and 12.2 $\pm$ 0.8 mmHg in the control group ($n = 5$), with no significant difference between the two groups.

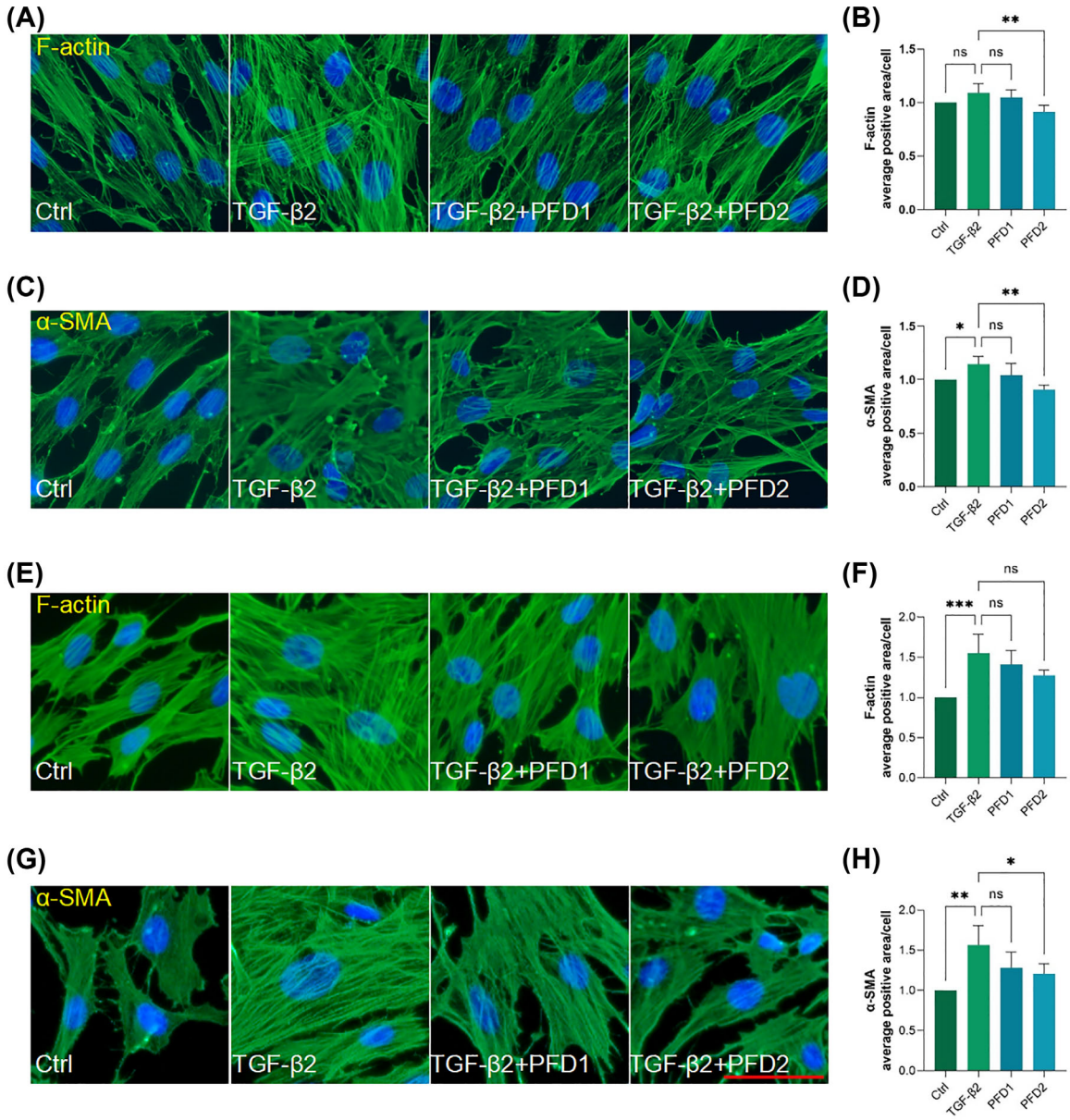

Figure 5. Immunofluorescence of cytoskeletal proteins in fibrotic TM cells with or without exposure to pirfenidone. (**A**, **C**) Representative fluorescence micrographs of F-actin (**A**) and α-SMA (**C**) in early-stage fibrotic TM cells of control, TGF-β2 (24 hours; 10 ng/mL), or TGF-β2 combined with PFD (24 hours; 0.1 mg/mL, 0.2 mg/mL). (**B**, **D**) Representative fluorescence micrographs of F-actin (**B**) and α-SMA (**D**) in late-stage fibrotic TM cells of control, TGF-β2 (48 hours; 10 ng/mL), or TGF-β2 (24 hours) and PFD (24 hours; 0.1 mg/mL, 0.2 mg/mL). *Scale bar*: 50 µm. (**E**–**H**) Analysis of F-actin (**E**, **F**) and α-SMA (G, H) average positive area per cell (total fluorescence area/total nuclei). $^{**}P < 0.01$, $^{***}P < 0.001$ ($n = 4$ images per group from four TM cell strains). PFD1, 0.1 mg/mL PFD; PFD2, 0.2 mg/mL PFD; ns, not significant.

On day 7, the mean IOP of the OHT group was 17.9 ± 1.8 mmHg and that of the control group was 12.4 ± 2.3 mmHg, a significant difference between the two groups ($P < 0.01$). On day 13, the mean value in the model group was 18.5 ± 1.5 mmHg, which was significantly higher than that in the control group ($P < 0.01$). On day 35, the IOP of the OHT group remained at 18.8 ± 1.2 mmHg ($P < 0.01$), indicating that Ad-TGF-$\beta2^{C226/228S}$ could successfully induce ocular hypertension in mice and maintain it for a long time (Fig. 7B).

PFD Reduced the IOP of the OHT Mouse Models

The baseline IOP values for the four groups (control, PBS, PFD, and LT) were 12.1 ± 1.5, 11.9 ± 0.4, 12.3

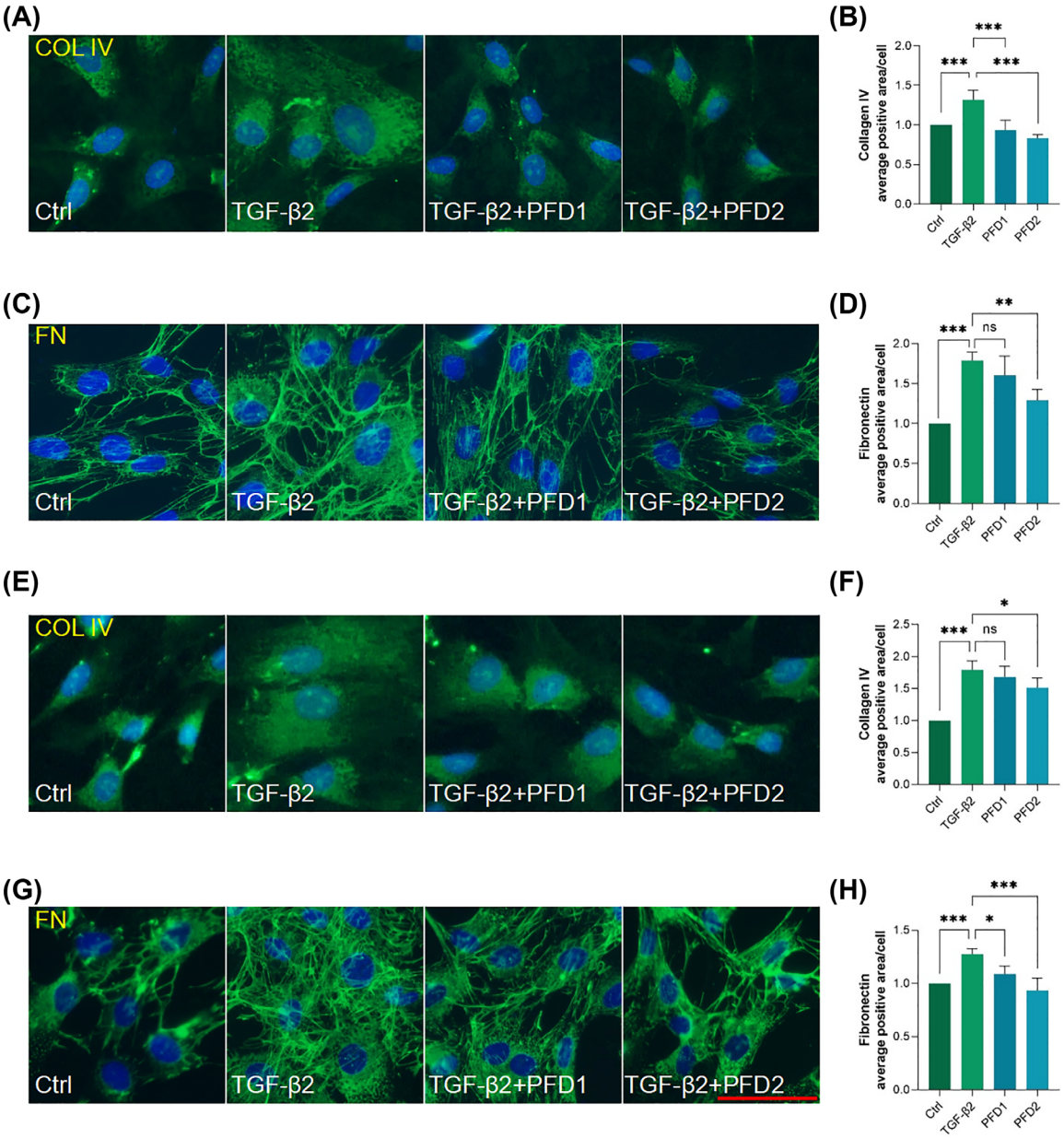

Figure 6. Immunofluorescence of extracellular matrix proteins in fibrotic TM cells with or without pirfenidone. (**A**, **C**) Representative fluorescence micrographs of COL IV (**A**) and FN (**C**) in early-stage fibrotic TM cells of control, TGF-β2 (24 hours; 10 ng/mL), or TGF-β2 combined with PFD (24 hours; 0.1 mg/mL, 0.2 mg/mL). (**B**, **D**) Representative fluorescence micrographs of COL IV (**B**) and FN (**D**) in late-stage fibrotic TM cells of control, TGF-β2 (48 hours; 10 ng/mL), or TGF-β2 (24 hours) and PFD (24 hours; 0.1 mg/mL, 0.2 mg/mL). *Scale bar*: 50 µm. (**E**–**H**) Analysis of COL IV (**E**, **F**) and FN (**G**, **H**) average positive area per cell (total fluorescence area/total nuclei). $^{**}P < 0.01$, $^{***}P < 0.001$ ($n = 4$ images per group from four TM cell strains). PFD1, 0.1 mg/mL PFD; PFD2, 0.2 mg/mL PFD; ns, not significant.

$\pm$ 0.8, and 11.7 $\pm$ 0.8 mmHg, respectively. No significant differences were observed among the four groups. On day 14, the IOP values for each group were 12.5 $\pm$ 1.9, 18.7 $\pm$ 1.0, 19.0 $\pm$ 1.1, and 19.3 $\pm$ 0.8 mmHg, respectively. The control group significantly differed from the other three groups ($P < 0.01$); however, there were no significant differences among the PBS, PFD, and LT groups. On day 17, IOP decreased in both the PFD and LT groups ($P < 0.05$), especially in the LT group. After day 20, IOP decreased significantly in both the PFD and LT groups ($P < 0.01$) (Fig. 8A); however, there was no significant difference in IOP reduction between the PFD and LT groups (Fig. 8B).

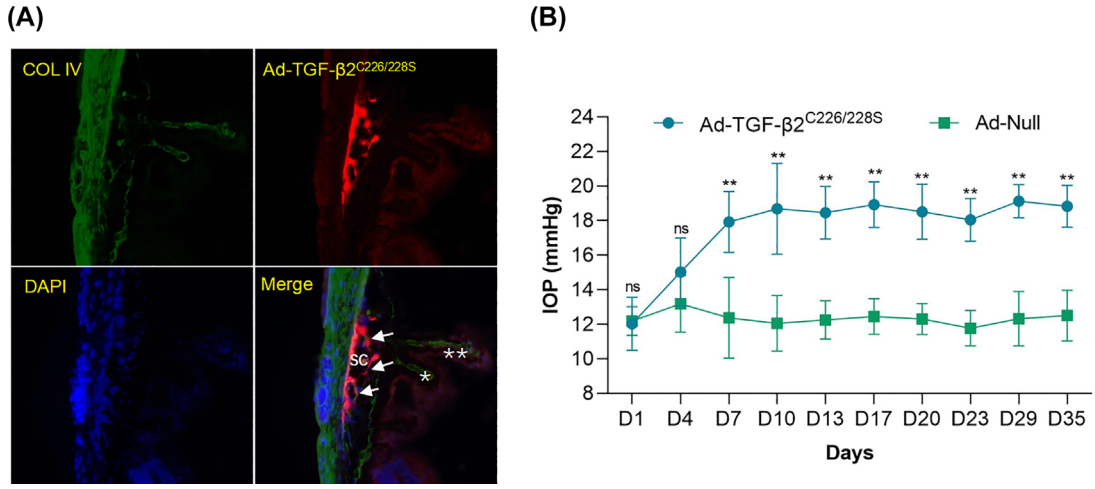

Figure 7. Ad-TGF-$\beta 2^{C226/228S}$–induced OHT mouse model. (**A**) Longitudinal section of a mouse eyeball on day 35. *Green fluorescence* indicates COL IV. *Red* indicates Ad-TGF-$\beta 2^{C226/228S}$. SC, Schlemm's canal; *ciliary body; **iris; →, TM. (**B**) Comparison of IOP between OHT mouse models and the control group. Ad-TGF-$\beta 2^{C226/228S}$ was used as the OHT model group ($n = 8$), and Ad-Null was used as the control group ($n = 5$). $^{**}P < 0.01$. ns, not significant.

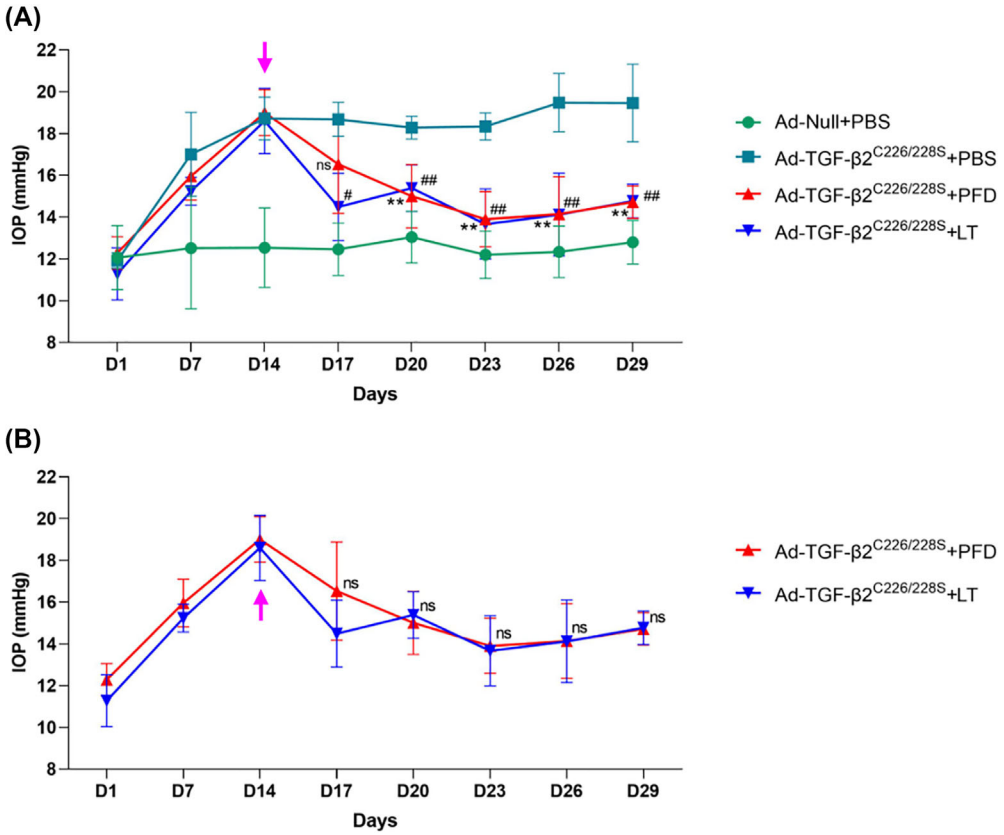

Figure 8. Effect of pirfenidone on the IOP in OHT mouse models. (**A**) PFD group ($n = 7$) and LT group ($n = 6$) compared to the PBS group ($n = 5$). The *arrow* indicates the time of administration. (**B**) Comparison between the PFD group and the LT group. The *arrow* indicates the time of administration. $^{**}P < 0.01$ (PFD group vs. PBS group), $\#\#P < 0.01$ (LT group vs. PBS group). LT, latanoprost eye drops; ns, not significant.

Discussion

The increase in TM outflow pathway resistance in the aqueous humor was the main cause of the elevated IOP observed in glaucoma patients.[21] Significant increases in ECM components, such as FN and COL IV, have been observed in TM tissues from patients with POAG,[22–24] and fibroblast proliferation was observed around the Schlemm's canal in POAG,[25,26] resulting in lumen narrowing. In the aqueous humor of patients with glaucoma, TGF-β has been shown to be significantly elevated, especially TGF-β2 in POAG.[3] This indicates that TM fibrosis is an important pathological process in the development of glaucoma. Therefore, we applied the highly effective antifibrotic drug PFD to the TM tissues and confirmed its substantial inhibitory effect on TGF-β2–induced fibrosis.

We found that PFD inhibits the proliferation of TM cells in a dose-dependent manner and that the safest concentration of PFD is less than 0.4 mg/mL for normal TM cells. PFD at or above 0.1 mg/mL significantly inhibited the proliferation of fibrotic TM cells (Fig. 2). Previous studies have found that the inhibitory effect of PFD on fibrotic cells is time and dose dependent.[27,28] In one study, the proliferation of rat fibroblasts[28] and TGF-β–induced primary human lung fibroblasts was inhibited by administering 0.1 mg/mL of PFD.[29] Based on the above, we determined that the safest and most effective concentration in vitro was 0.2 mg/mL, which was within the safe concentration of normal TM cells and could inhibit the proliferation of fibrotic TM cells. We used 0.1 mg/mL as the reference concentration value.

F-actin stress fibers are present in higher numbers in TM cells isolated from POAG eyes than in normal TM cells,[30,31] and disorganized F-actin fibers spontaneously form CLANs, resulting in increased stiffness of TM cells.[32] Steroid treatment of normal and glaucomatous TM cells results in ultrastructural changes, including a significant increase in the formation of CLANs, as well as cell and nuclear enlargement.[8] Our results are consistent with previous findings. The cell body of late-stage fibrotic TM cells was larger than that in the early stages. TM cells appeared as denser groups of disordered and overlapping actin bundles, and the average positive area per cell was significantly increased in late fibrosis. This may be related to the duration of exposure to TGF-β2. Surprisingly, in this study, the expression of F-actin protein was not significantly changed after TGF-β2 treatment of TM cells. We hypothesized that TGF-β2 stimulation resulted in an enlargement of TM cells and primarily affected the structural arrangement of F-actin, with a secondary effect on the expression of F-actin. TGF-β2 regulates the expression of F-actin, mainly through the Rho–Rho-associated kinase (ROCK) pathway, which induces disorder and elongation, resulting in the formation of CLANs and thereby increasing cell stiffness.[33] Therefore, we speculate that PFD is not involved in the Rho–ROCK pathway regulating F-actin but can regulate the structure in other ways, the specific mechanisms of which are unclear.

In this study, α-SMA, COL IV, and FN were significantly overexpressed following TGF-β2 induction, which was consistent with the results of previous studies.[33–36] Western blot and immunofluorescence analysis showed that PFD significantly inhibited the overexpression of α-SMA, COL IV, and FN and reduced the average positive area per cell. In addition, we found that the effect of PFD was more pronounced in reducing ECM deposition than in remodeling the cytoskeleton, which could be involved in several mechanisms. Studies have shown that PFD affects the proliferation of fibrotic cells and the expression of fibrotic protein–related genes. Conte et al.[29] found that PFD reduces the proliferation of human lung fibroblast by inhibiting TGF-β–induced phosphorylation of Smad3, p38, and Akt. Additionally, PFD reduces mRNA and protein levels of α-SMA and procollagen type I (COL I), thereby attenuating TGF-β–mediated fibroblast to myofibroblast differentiation. PFD regulates the Wnt/GSK-3β/β-catenin signaling pathway to inhibit bleomycin-induced overexpression of the mRNA and protein of α-SMA, collagen III (COL III), and FN in mouse lung,[37] and it inhibits proliferation of hepatoma cells and promotes apoptosis.[38] PFD attenuates TGF-β–induced FN and α-SMA expression in fibroblasts from ocular Tenon's capsule and orbital adipose tissue.[16] PFD also affects ECM deposition at the protein level. It upregulates the levels of matrix metalloproteinases (MMPs)/tissue inhibitors of metalloproteinases (TIMP), leading to promotion of ECM degradation.[39] Additionally, it downregulates the expression of heat shock protein 47 (HSP47), inhibiting procollagen processing, assembly, and secretion.[39] In lung fibroblasts, it also affects collagen triple helix repeat containing 1 (CTHR1), inhibiting fibronectin migration and collagen contraction.[40] Various mechanisms are involved in the regulation of fibrosis by pirfenidone. Further exploration of the specific mechanism of anti-trabecular meshwork fibrosis is required.

Ad-TGF-$\beta2^{C226/228S}$ induced ocular hypertension in mice. This could be because, similar to the case for POAG, TGF-β2 changes the cytoskeleton in the TM and increases ECM synthesis and deposition.[41] It

has been confirmed that Ad-TGF-$\beta 2^{C226/228S}$ increases IOP in mice,[17,42,43] and α-SMA, COL-I, and FN are significantly overexpressed.[34] Consistently, this study confirmed that Ad-TGF-$\beta 2^{C226/228}$ specifically targeted the TM in mice, with minimal effect on other tissues.

In this study, 0.4% PFD–HPMC eye drops decreased IOP in OHT mouse models on day 17, although the decrease was not as pronounced as with LT. These results suggest that PFD may require a longer duration to effectively reverse TM fibrosis in vivo. After day 17, IOPs of the mice decreased significantly, indicating that 0.4% PFD–HPMC eye drops could enter the anterior chamber and reach an effective concentration to play an anti-TM fibrosis role in vivo. Latanoprost eye drops are the first-line drug for POAG and mainly reduce IOP by enhancing the uveoscleral outflow pathway. However, the results of this experiment showed that there was no significant difference in the IOP-lowering effect between the PFD and LT groups, suggesting that PFD can effectively reduce IOP by enhancing the TM outflow pathway of the aqueous humor in Ad-TGF-$\beta 2^{C226/228S}$–induced OHT mouse models, and its specific mechanism may be consistent with our in vitro studies. However, these results must be further confirmed via tissue section to detect the related proteins. Due to time constraints, we were unable to perform this step, which is a limitation of our study. Additionally, further investigation is warranted to determine whether there is a potential for IOP rebound after PFD treatment targeting TM fibrosis is discontinued. Our findings indicate that using PFD to target the regulation of TM fibrosis could be an effective strategy for managing OHT.

In conclusion, our study demonstrated that pirfenidone inhibited fibrotic TM cell proliferation, reshaped the cytoskeleton of fibrotic TM cells, and reduced ECM deposition in a dose-dependent manner. We propose that pirfenidone reduces IOP by increasing the TM outflow pathway of the aqueous humor, thus providing a potential new approach to the treatment of glaucoma.

Acknowledgments

The authors thank Gu Jianjun and his team at Zhongshan Ophthalmology Center of Sun Yat-Sen University for assistance with corneoscleral rings. The authors also thank their colleagues in the research group for their help.

Supported by a grant from the Natural Science Foundation of Guangdong Province (2021A1515010604).

Disclosure: **X. Zhu**, None; **B. Zeng**, None; **C. Wu**, None; **Z. Chen**, None; **M. Yu**, None; **Y. Yang**, None

References

1. Belamkar A, Harris A, Oddone F, Verticchio Vercellin A, Fabczak-Kubicka A, Siesky B. Asian race and primary open-angle glaucoma: where do we stand? *J Clin Med*. 2022;11:2486.
2. Kang JM, Tanna AP. Glaucoma. *Med Clin North Am*. 2021;105:493–510.
3. Prendes MA, Harris A, Wirostko BM, Gerber AL, Siesky B. The role of transforming growth factor beta in glaucoma and the therapeutic implications. *Br J Ophthalmol*. 2013;97:680–686.
4. Tripathi RC, Li J, Chan WF, Tripathi BJ. Aqueous humor in glaucomatous eyes contains an increased level of TGF-$\beta 2$. *Exp Eye Res*. 1994;59:723–727.
5. Inatani M, Tanihara H, Katsuta H, Honjo M, Kido N, Honda Y. Transforming growth factor-β_2 levels in aqueous humor of glaucomatous eyes. *Graefes Arch Clin Exp Ophthalmol*. 2001;239:109–113.
6. Ochiai Y, Ochiai H. Higher concentration of transforming growth factor-beta in aqueous humor of glaucomatous eyes and diabetic eyes. *Jpn J Ophthalmol*. 2002;46:249–253.
7. Raghunathan VK, Morgan JT, Park SA, et al. Dexamethasone stiffens trabecular meshwork, trabecular meshwork cells, and matrix. *Invest Ophthalmol Vis Sci*. 2015;56:4447–4459.
8. Bermudez JY, Montecchi-Palmer M, Mao W, Clark AF. Cross-linked actin networks (CLANs) in glaucoma. *Exp Eye Res*. 2017;159:16–22.
9. Tanito M, Kaidzu S, Takai Y, Ohira A. Association between systemic oxidative stress and visual field damage in open-angle glaucoma. *Sci Rep*. 2016;6:25792.
10. Liton PB, Challa P, Stinnett S, Luna C, Epstein DL, Gonzalez P. Cellular senescence in the glaucomatous outflow pathway. *Exp Gerontol*. 2005;40:745–748.
11. Lin CW, Sherman B, Moore LA, et al. Discovery and preclinical development of netarsudil, a novel ocular hypotensive agent for the treatment of glaucoma. *J Ocul Pharmacol Ther*. 2018;34:40–51.
12. Lancaster LH, de Andrade JA, Zibrak JD, et al. Pirfenidone safety and adverse event management in idiopathic pulmonary fibrosis. *Eur Respir Rev*. 2017;26:170057.
13. Lin X, Yu M, Wu K, Yuan H, Zhong H. Effects of pirfenidone on proliferation, migration, and col-

lagen contraction of human Tenon's fibroblasts in vitro. *Invest Ophthalmol Vis Sci*. 2009;50:3763–3770.
14. Wang J, Yang Y, Xu J, Lin X, Wu K, Yu M. Pirfenidone inhibits migration, differentiation, and proliferation of human retinal pigment epithelial cells in vitro. *Mol Vis*. 2013;19:2626–2635.
15. Yang Y, Ye Y, Lin X, Wu K, Yu M. Inhibition of pirfenidone on TGF-beta2 induced proliferation, migration and epithelial-mesenchymal transition of human lens epithelial cells line SRA01/04. *PLoS One*. 2013;8:e56837.
16. Stahnke T, Kowtharapu BS, Stachs O, et al. Suppression of TGF-β pathway by pirfenidone decreases extracellular matrix deposition in ocular fibroblasts in vitro. *PLoS One*. 2017;12:e0172592.
17. McDowell CM, Tebow HE, Wordinger RJ, Clark AF. Smad3 is necessary for transforming growth factor-beta2 induced ocular hypertension in mice. *Exp Eye Res*. 2013;116:419–423.
18. Hernandez H, Roberts AL, McDowell CM. Nuclear factor-kappa beta signaling is required for transforming growth factor beta-2 induced ocular hypertension. *Exp Eye Res*. 2020;191:107920.
19. Keller KE, Bhattacharya SK, Borras T, et al. Consensus recommendations for trabecular meshwork cell isolation, characterization and culture. *Exp Eye Res*. 2018;171:164–173.
20. Stamer WD, Clark AF. The many faces of the trabecular meshwork cell. *Exp Eye Res*. 2017;158:112–123.
21. Costagliola C, dell'Omo R, Agnifili L, et al. How many aqueous humor outflow pathways are there? *Surv Ophthalmol*. 2020;65:144–170.
22. Tektas OY, Lutjen-Drecoll E. Structural changes of the trabecular meshwork in different kinds of glaucoma. *Exp Eye Res*. 2009;88:769–775.
23. Okamoto M, Nagahara M, Tajiri T, Nakamura N, Fukunishi N, Nagahara K. Rho-associated protein kinase inhibitor induced morphological changes in type VI collagen in the human trabecular meshwork. *Br J Ophthalmol*. 2020;104:392–397.
24. Tovar-Vidales T, Roque R, Clark AF, Wordinger RJ. Tissue transglutaminase expression and activity in normal and glaucomatous human trabecular meshwork cells and tissues. *Invest Ophthalmol Vis Sci*. 2008;49:622–628.
25. Hamanaka T, Sakurai T, Fuse N, Ishida N, Kumasaka T, Tanito M. Comparisons of Schlemm's canal and trabecular meshwork morphologies between juvenile and primary open angle glaucoma. *Exp Eye Res*. 2021;210:108711.
26. Hamanaka T, Matsuda A, Sakurai T, Kumasaka T. Morphological abnormalities of Schlemm's canal in primary open-angle glaucoma from the aspect of aging. *Invest Ophthalmol Vis Sci*. 2016;57:692–706.
27. Wei Q, Kong N, Liu X, et al. Pirfenidone attenuates synovial fibrosis and postpones the progression of osteoarthritis by anti-fibrotic and anti-inflammatory properties in vivo and in vitro. *J Transl Med*. 2021;19:157.
28. Zhang X, Zhang J, Liu Y, et al. Pirfenidone inhibits fibroblast proliferation, migration or adhesion and reduces epidural fibrosis in rats via the PI3K/AKT signaling pathway. *Biochem Biophys Res Commun*. 2021;547:183–191.
29. Conte E, Gili E, Fagone E, Fruciano M, Iemmolo M, Vancheri C. Effect of pirfenidone on proliferation, TGF-β-induced myofibroblast differentiation and fibrogenic activity of primary human lung fibroblasts. *Eur J Pharm Sci*. 2014;58:13–19.
30. Clark AF, Miggans ST, Wilson K, Browder S, McCartney MD. Cytoskeletal changes in cultured human glaucoma trabecular meshwork cells. *J Glaucoma*. 1995;4:183–188.
31. Hoare M-J, Grierson I, Brotchie D, Pollock N, Cracknell K, Clark AF. Cross-linked actin networks (CLANs) in the trabecular meshwork of the normal and glaucomatous human eye in situ. *Invest Ophthalmol Vis Sci*. 2009;50:1255–1263.
32. Peng M, Rayana NP, Dai J, et al. Cross-linked actin networks (CLANs) affect stiffness and/or actin dynamics in transgenic transformed and primary human trabecular meshwork cells. *Exp Eye Res*. 2022;220:109097.
33. Buffault J, Brignole-Baudouin F, Reboussin É, et al. The dual effect of rho-kinase inhibition on trabecular meshwork cells cytoskeleton and extracellular matrix in an in vitro model of glaucoma. *J Clin Med*. 2022;11:1001.
34. Kasetti RB, Maddineni P, Kodati B, Nagarajan B, Yacoub S. Astragaloside IV attenuates ocular hypertension in a mouse model of TGFβ2 induced primary open angle glaucoma. *Int J Mol Sci*. 2021;22:12508.
35. Tellios N, Belrose JC, Tokarewicz AC, et al. TGF-β induces phosphorylation of phosphatase and tensin homolog: implications for fibrosis of the trabecular meshwork tissue in glaucoma. *Sci Rep*. 2017;7:812.
36. Medina-Ortiz WE, Belmares R, Neubauer S, Wordinger RJ, Clark AF. Cellular fibronectin expression in human trabecular meshwork and induction by transforming growth factor-β2. *Invest Ophthalmol Vis Sci*. 2013;54:6779–6788.
37. Lv Q, Wang J, Xu C, Huang X, Ruan Z, Dai Y. Pirfenidone alleviates pulmonary fibrosis in vitro

and in vivo through regulating Wnt/GSK-3β/β-catenin and TGF-β1/Smad2/3 signaling pathways. *Mol Med*. 2020;26:49.
38. Zou W-J, Huang Z, Jiang T-P, et al. Pirfenidone inhibits proliferation and promotes apoptosis of hepatocellular carcinoma cells by inhibiting the Wnt/β-catenin signaling pathway. *Med Sci Monit*. 2017;23:6107–6113.
39. Ruwanpura SM, Thomas BJ, Bardin PG. Pirfenidone: molecular mechanisms and potential clinical applications in lung disease. *Am J Respir Cell Mol Biol*. 2020;62:413–422.
40. Jin J, Togo S, Kadoya K, et al. Pirfenidone attenuates lung fibrotic fibroblast responses to transforming growth factor-β1. *Respir Res*. 2019;20:119.
41. Han H, Wecker T, Grehn F, Schlunck G. Elasticity-dependent modulation of TGF-beta responses in human trabecular meshwork cells. *Invest Ophthalmol Vis Sci*. 2011;52:2889–2896.
42. Mody AA, Millar JC, Clark AF. ID1 and ID3 are negative regulators of TGFβ2-induced ocular hypertension and compromised aqueous humor outflow facility in mice. *Invest Ophthalmol Vis Sci*. 2021;62:3.
43. Shepard AR, Millar JC, Pang I-H, Jacobson N, Wang W-H, Clark AF. Adenoviral gene transfer of active human transforming growth factor-β2 elevates intraocular pressure and reduces outflow facility in rodent eyes. *Invest Ophthalmol Vis Sci*. 2010;51:2067–2076.